Chapter 1

Introduction

1.1 History of Breadboards

The breadboard has been a staple substrate for electronic construction over the last century. At the dawn of a growing interest in amateur radio, resourceful tinkerers used planks of wood to secure and ruggedize their electrical handiwork. Conductive nodes, such as nails or copper rails, were driven into the non-conductive boards, providing anchors and contact points that were electrically isolated from the rest of the circuit. Components were soldered or wire-wrapped to the nodes, and sometimes secured by non-energized nails or screws. This construction technique provided a lot of artistic freedom in circuit construction, but was time consuming and required relatively heavy hand tools such as a hammer or drill.

1.2 Modern Breadboards

The solderless breadboard is the canonical tool given to students taking introductory courses in the field. Rather than driving nodes into arbitrary locations, component leads are inserted into contact points arranged on a grid that allow rapid semi-rigid construction of circuits with no other tools. The layout of a solderless breadboard is designed to be compatible with a plethora of powerful integrated circuits, enabling complex electronic designs. Modern solderless breadboards have come a long way from their namesake wooden ancestors, but there is still room for improvement.

The intent of breadboarding is to physically realize a circuit. Often, this involves designing or using a reference schematic to guide construction, but circuit improvisation is

not uncommon. A meticulous breadboarder can successfully realize a circuit without error by correctly placing components and jumper wires - taking care not to introduce undesired 'parasitic' components. However, for the uninitiated it is difficult to justify the additional time and care required to plan and build. Inserting components and jumper wires into contact points is straightforward, but poor contacts, broken wires (inside insulation), and misinserting leads can plague designers for hours on end and potentially destroy components. The shortcomings of solderless breadboards lie entirely within the art of breadboarding. Breadboarding is a skill that is learned over time, but small errors can lead to excessive frustration and turn students off to the field.

To satisfy the requirements of the Masters in Engineering program, I propose a solution to some of the issues with the solderless breadboard.

A confident linkage between the the electrical and mechanical domains is required to construct a circuit. On larger scales, the mechanical structures (eg. contacts, wires, components) that create electrical circuits are visible in plain sight. It is simple and reliable, then, to determine the circuit representation of a mechanical structure that has no hidden connections. Breadboards often obscure connections due to their construction. The regular nature of a breadboard, a grid of contact points arranged in rails, makes it difficult to keep track of which rail is connected to what circuit node. When combined with the opaque nature of most components and the poor reliability of breadboard contacts, visually verifying complex circuits on a breadboard becomes infeasible. Many of the inherent problems with breadboards stem from this open-loop nature of breadboarding, where visual cues are not enough to determine the electrical circuit from the mechanical structure. A symptom of open-loop construction techniques is a mismatch between the mental model and the physical realization of the system at hand. I seek to close this loop by designing and implementing a circuit-sensing breadboard.

1.3 Proposed Solution

A hardware test-bench was constructed to interface with 8 rails on a breadboard. The test-bench is composed of a pcb-mounted breadboard, an ADC and DAC multiplexing board, a microcontroller development board, firmware to control sampling and stimulating the breadboard, and software to stream the sampling data to a computer for display. Since software

is faster to prototype with, the theoretical circuit topology work was first implemented in software. A circuit simulator test-bench was written to provide the circuit-sensing algorithm in development with data. This test-bench allows the circuit-sensing algorithm to probe, stimulate, and ground every node of a randomly generated circuit, as if the circuit were built on a breadboard attached to the hardware test bench mentioned above. The software test-bench also had the ability to print out a circuit network solution to a schematic display.

1.4 Implementation to Date

Made the software test bench, an 8-rail hardware test bench, and got the network sensing algorithm working for resistors with resistance between 100 and 5K Ω.

Chapter 2

Theory

The design of a Network Sensing Algorithm requires an understanding of the networks to be analyzed. In this thesis, the networks of interest are composed of three circuit elements: resistors, capacitors, and inductors. The constitutive relations for these electrical circuit elements relate the voltage across an element to the current passing through it as a function of time. In this application, it is useful to reinterpret the constitutive relations as a function of frequency by taking the Laplace Transform.

2.1 RLC Elements

Constitutive relations: $v = iR, v = L\frac{di}{dt}$, and $i = C\frac{dv}{dt}$

2.2 Frequency Domain Perspective

Laplace transform of:

$v = iR, v = L\frac{di}{dt}$, and $i = C\frac{dv}{dt}$

$V = IR, V = LsI, I = CsV$

Impedance:

$Z_R = R, Z_L = Ls, Z_C = \frac{1}{Cs}$

2.3 Network Analysis

KVL KCL

Chapter 3

Network Sensing Algorithm

Given access to the set of nodes in an electrical network, the objective of a network sensing algorithm is to determine the set of branches and the elements that compose them. In order to illustrate how a network sensing algorithm operates, it is necessary to begin with a simple example and then build in complexity.

3.1 Grounding Clause

The ability to ground arbitrary nodes of a network greatly simplifies the process of analyzing and reverse-engineering a network. The NSA relies on the ability to shrink the effective network by conglomerating nodes into the ground node.

3.2 Two Node Network

Take the example of a network with two nodes below:

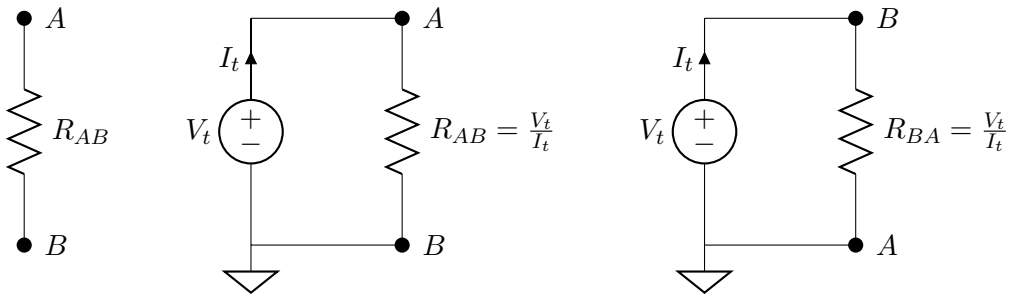

Figure 3-1: Finding R_{AB} in a two node network

In the case of a resistive network with two nodes, there is only one possible branch in the network and thus one possible element to characterize. From elementary circuit theory, the resistance between two nodes equal to the voltage across the nodes divided by the current through the nodes when power is applied. Here, the resistance R_{AB} is found by placing a test voltage V_t across the nodes and measuring the resulting current, I_t, then taking the ratio $\frac{V_t}{I_t}$. This measurement is called the driving point impedance [1]. If there are no circuit elements between the two nodes, the driving point impedance test will find zero current in the test voltage source, resulting in an infinite resistance between two nodes. An infinite resistance between two nodes in a circuit indicates that there are no elements in that branch of the network. Thus, the network can subsequently be simplified by removing that branch from the network.

3.3 Three Node Network

A resistive network with two nodes is simple, but provides an introduction to the methodology used in analyzing larger networks. In the case of a resistive network with three nodes, it is insufficient to utilize driving point impedance measurements alone, because each node has more than one path to any other node.

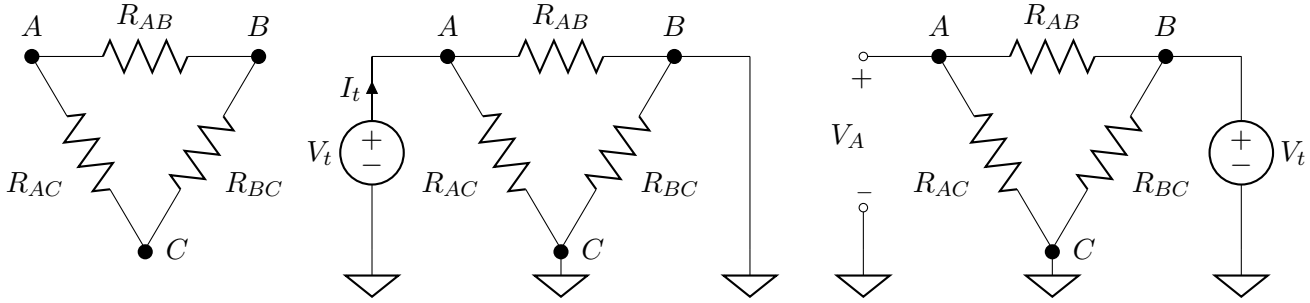

Figure 3-2: Finding R_{AB} in a three node network

Consider a resistive network with three nodes: A, B, and C. In order to determine the resistance in branch AB, the driving point impedance at node A is measured with nodes B and C grounded. This provides the resistance of the parallel combination of the branches with an endpoint at node A,

[1] To measure a driving point impedance, a test voltage is applied between the node of interest and ground, and the resulting current in the voltage source is measured. The driving point impedance is then computed by dividing the test voltage by the resulting current.

$R_{A_{||}} = R_{AB}||R_{AC}$. [2] Next, a test voltage source is applied to node B, node C is grounded, and the voltage at node A, V_A, is observed. $V_A = V_t \frac{R_{AC}}{R_{AB} + R_{AC}} = V_t \frac{R_{AB}||R_{AC}}{R_{AB}} = V_t \frac{R_{A_{||}}}{R_{AB}}$
The branch resistance of interest, R_{AB} is calculated using the known quantities V_t, $V_{A||}$, and V_A. $R_{AB} = V_t \frac{R_{A||}}{V_A}$
This procedure is repeated for the remaining branches to determine the entire network.

3.4 N Node Network

A resistive network with any number of nodes can be reduced to a resistive network with three nodes by grounding the nodes that are not of interest. The resulting network does not modify the branch of interest, but connects the remaining branches attached to the nodes of interest in parallel. This collapses the network into a three node network or three branch equivalent circuit. Consider a resistive network with five nodes: A-E. To determine

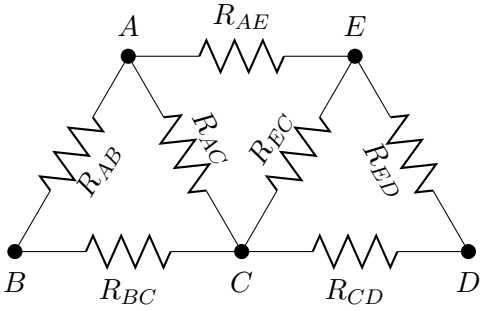

Figure 3-3: Five node network

the resistance between nodes A and E, the network is reduced to a three-node network by connecting all nodes except nodes A and E to ground. The three resistances of the branches that remain are R_{AE}, $R_{AB}||R_{AC}$, and $R_{EC}||R_{ED}$. The reduced network is then solved using the three node network method, and this procedure is repeated for all branches in the network.

[2] $R_1||R_2 = \frac{R_1 R_2}{R_1 + R_2}$

3.5 Element Identification

Networks composed of elements with complex impedance can be analyzed with the same algorithm. By replacing the test DC voltage sources with AC voltage sources, the imaginary reactance of capacitors and inductors can be measured in addition to the real resistance of resistors.

3.5.1 From Resistance to Impedance

Chapter 2 described the use of the Laplace Transform to characterize the behavior of circuit elements in the frequency domain. Here, frequency-domain complex impedance is useful for identifying circuit elements based on the change in branch impedance over inputs of various frequencies.

MAKE NOTE ABOUT USING THE AMPLITUDE OF THE MEASURED SIGNALS

3.5.2 Parallel RLC Branches

To determine if there are multiple element types [in parallel] between two nodes, we can select a few frequencies to scan through and analyze the resulting change in impedance.

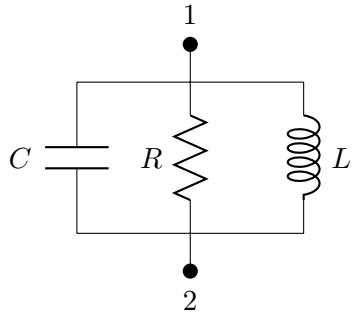

Figure 3-4: Example RLC Tank Circuit

The impedance of a parallel RLC 'tank' circuit can be characterized and analyzed over all frequencies.

$$Z_C = \frac{1}{j\omega C} \qquad Z_R = R \qquad Z_L = j\omega L \tag{3.1}$$

$$Z_{RLC} = Z_C||Z_R||Z_L = \frac{1}{j\omega C + \frac{1}{R} + \frac{1}{j\omega L}} = \frac{j\omega RL}{-\omega^2 RLC + j\omega L + R} \tag{3.2}$$

Z_{RLC} has a zero at $\frac{1}{RL}$ and two poles at $\frac{-L^{+}_{-}\sqrt{L^2+4R^2LC}}{-2RLC}$

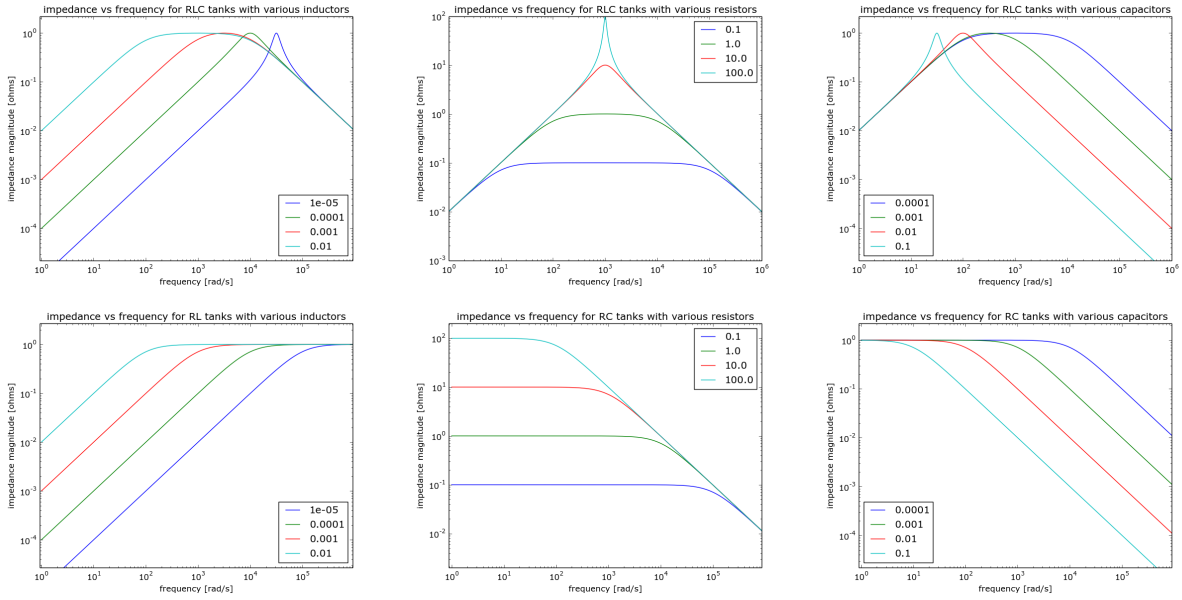

If we look at the plots above, we can see that varying the resistance changes the maximum impedance over all frequencies, varying the inductance drops the asymptotic impedance at low frequencies, and varying the capacitance drops the asymptotic impedance at high frequencies. We can imagine there are three regimes on the impedance vs frequency plot that divide the operation of an RLC tank into three elements:

When the slope is +1, the tank behaves like an inductor

$L = |Z|/(j\omega)$.

When the slope is -1, the tank behaves like a capacitor

$C = j\omega|Z|$.

When the slope is 0, the tank behaves like a resistor

$R = |Z|$.

3.5.3 Finite Difference Stencil

To reliably determine the regions of effective resistance, inductance, and capacitance, the slope of the $log|Z_{nm}|$ vs. $log(\omega)$ is computed via the Midpoint Method. The Midpoint Finite Difference Stencil takes the two points on either side of the point of interest and computes the slope between them.

Z'[n]=$\frac{1}{2}$(Z[n+1]-Z[n-1]).

3.5.4 Component Value Calculation

Once the regions of the impedance plot are identified and assigned to component, the component value is calculated for each sample taken on the impedance plot:

$R = Z[\omega]$

$L = \frac{Z[\omega]}{\omega}$

$C = \frac{1}{\omega Z[\omega]}$

The resulting resistances, inductances, and capacitances are averaged to counter noisy data.

3.6 Reconstructing the Network

With a record of all of the elements and their connections in the network, the network is reconstructed.

Chapter 4

Simulation

A simulation was built to test the Network Sensing Algorithm before embarking on hardware design. In addition to the rapid prototyping cycle, the implementation of NSA and automated schematic drawing were directly used later on. The simulation generates random networks of resistors, inductors, and capacitors, and proceeds to analyze and reconstruct the network using NSA.

4.1 NgSpice and Netlists

The open source software package NgSpice was used to simulate the networks and test circuits applied to the network. NGspice operates on text files called netlists, where each component in the network is specified on a single line. An example netlist is shown below.

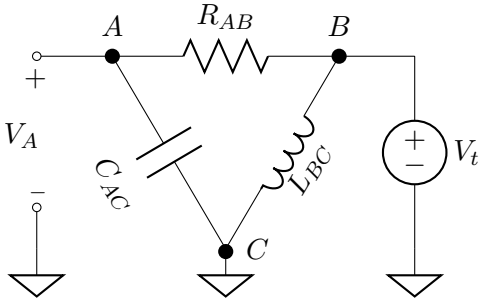

Figure 4-1: Five node network

```
fiveNodeNetlist
Vt 0 B 1
```

```
Rab A B 10k
Cac A C 1e-6
Lbc B C 1e-3
Vcg 0 C 0
.control
op
print(v(A))
.endc
.end
```

The first letter of each element line designates the element to simulate:

`V start stop value`→ Voltage Source between `start` and `stop` nodes, `value` Volts [V]

`R start stop value`→ Resistor between `start` and `stop` nodes, `value` Ohms [Ω]

`L start stop value`→ Inductor between `start` and `stop` nodes, `value` Henries [H]

`C start stop value`→ Capacitor between `start` and `stop` nodes, `value` Farads [F]

Node 0 is always designated as ground, and all simulations require a ground node.

The control commands are as follows:

`op` → Operating Point Simulation `print()` → Print the relevant data passed as an argument

`v(N)` → The voltage at node N `i(E)` → The current through element E

4.2 Methods

The NSA simulator was written in python and uses the methods below.

4.2.1 Generate Random Netlist

`writeRandomNet(netlist,num,elements):`

Generates `num`-node random graph with no self-linking nodes (symmetric matrix with zeros on the diagonal) for each `[elements]` type (R,L,C). Subsequently assigns random values between two realistic limits for each element and writes the network to netlist `netlist`. 1-1k ohms, 10nF-10uF, 100uH-100mH.

When writing the capacitive and inductive elements, care must be taken to prevent a DC operating point simulation from failing. The infinite resistance across a capacitor and

zero resistance across an inductor are responsible for DC operating point simulation failure, and can be fixed by including a small resistor in series with inductors and a large resistor in parallel with capacitors.

`L0 1 2 1mH`	→	`L0 1 tl0 1mH` `Rl0 tl0 2 1e-5`	`C0 1 2 1e-6F`	→	`C0 1 2 1e-6F` `Rc0 1 2 1e8`

4.2.2 Inserting Voltage Sources, Grounds and Probes

`insertProbe2(target,nodes,groundNodes,probes,source='DC'):`

Inserts a 1V voltage source from ground to each node in `[nodes]`, grounds each node in `[groundNodes]`, and adds a voltage print statement for each node in `[probes]`. By default, the voltage sources are written as DC sources, but if 'AC' is passed into the last argument the sources are written as AC sources and the AC control statement is added.

`AC dec 1 1 100000`

Which runs a small-signal AC simulation and returns the amplitudes of the resulting voltage and current waveforms, one sample point per decade from 1Hz to 100kHz.

4.2.3 Run Simulation

`def runSim(target,results,source='DC'):`

Makes a system call to NgSpice in batch mode with netlist `target` and outputs the result to text file `results`. The last argument indicates how to parse the resulting data, as NgSpice returns DC data in the following format:

```
No.  of Data Rows :  1
i(v) = -1.18295e-01
v(5) = 2.532846e-07
```

and AC data is returned in this format:

```
No.  of Data Rows :  6
mynetlist
AC Analysis Sun Aug 30 18:35:07 2015
--------------------------------------------------------------------------------
Index frequency i(v)
--------------------------------------------------------------------------------
0 1.000000e+00 -1.72598e+00, 3.978810e+02
```

```
1 1.000000e+01 -1.58689e-01, 3.978827e+01
2 1.000000e+02 -1.43015e-01, 3.974287e+00
3 1.000000e+03 -1.42859e-01, 3.520201e-01
4 1.000000e+04 -1.42857e-01, -4.18884e-01
5 1.000000e+05 -1.42857e-01, -4.58275e+00


mynetlist
AC Analysis Sun Aug 30 18:35:07 2015
--------------------------------------------------------------------------------
Index frequency v(3)
--------------------------------------------------------------------------------
0 1.000000e+00 1.000000e+00, 0.000000e+00
1 1.000000e+01 1.000000e+00, 0.000000e+00
2 1.000000e+02 1.000000e+00, 0.000000e+00
3 1.000000e+03 1.000000e+00, 0.000000e+00
4 1.000000e+04 1.000000e+00, 0.000000e+00
5 1.000000e+05 1.000000e+00, 0.000000e+00
```

4.2.4 Print Matrix

`def printMatrix(m):` Prints matrix `m` in nice command-line output.

4.3 Executing NSA

4.3.1 Calculate $Z_{n||}(f)$

$Z_{n||}(f)$ is found by grounding all nodes except for node n and adding a voltage source to that node, then taking the ratio of the amplitudes of the resulting current into the node of interest and the voltage source.

4.3.2 Calculate $V_n(f)$

$V_n(f)$ is found by grounding all nodes except for nodes n and m, adding a voltage source to node m, and measuring the amplitude of the voltage at node n.

4.3.3 Calculate $Z_{nm}(f)$

$Z_{nm}(f)$ is calculated by the ratio of $Z_{n||}(f)$ to $V_n(f)$ scaled by V_t. In the case of this simulation, V_t is one.

4.3.4 Finite Difference

4.3.5 Element Identification

4.3.6 Network Reconstruction

4.4 Output to JSON

Blah Blah

4.5 D3?

???? maybe

Chapter 5

Hardware

Block diagram / Schematic

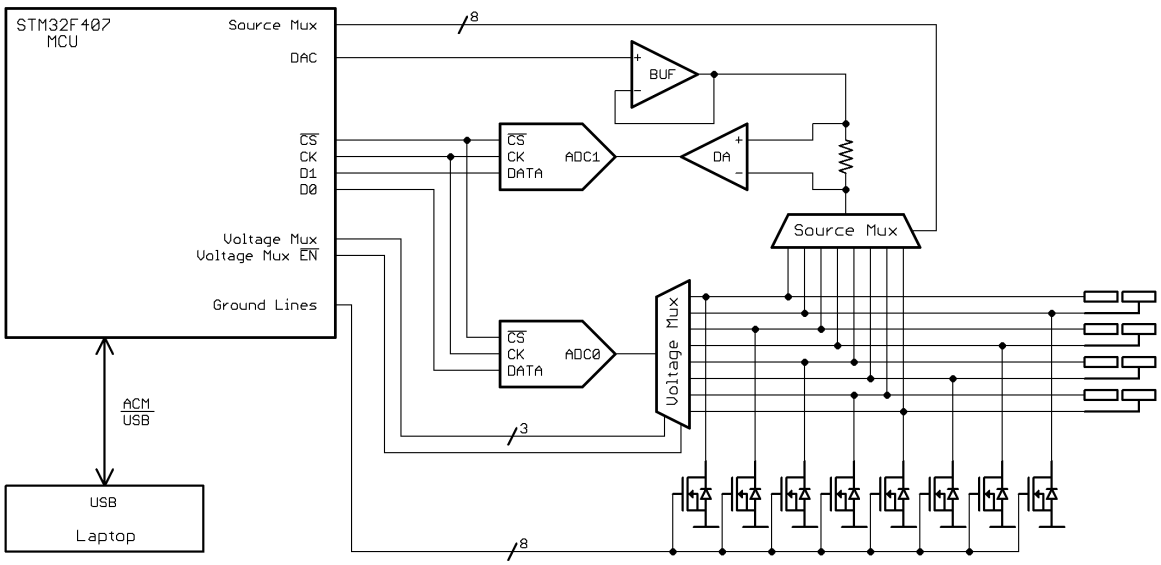

5.1 Low Cost

Keeping the cost of production low makes butterboard accessible to the largest population of people. Using multiplexed ADCs where possible keeps the cost down by reducing the quantity of high price-tag components, like ADCs.

5.2 Node Voltage Reading

Although the STM32F407 has three onboard 12-bit A/D converters, their specifications are lacking. Each is able to sample at 2MSPS, and it's possible to interleave them to attain a sampling rate of 6MSPS or higher if you're willing to throw away bits. The total unadjusted error (offset error, gain error, differential linearity error, and integral linearity error) is between ±2 LSB and ±5 LSB. With a minimum of ±2 LSB's of error, the lowest significant two bits in the 12-bit A/D are virtually useless. Another specification to consider is the input circuitry to the ADC. The input circuitry to the ADC while it's in tracking mode looks like a 6KΩ resistor charging a 4pF capacitor. This puts a pole at 6.6MHz, causing .3% error in measurement at 100KHz, 3% error in measurement at 1MHz, and 7% at 3MHz. When sampling at the maximum sample rate of 6MSPS, the ADC's input network begins to introduce significant error. Granted, it's likely that there will be an alternative bandwidth bottleneck, this is still a metric of concern. [DM00037051.pdf, pages 133-134]

An ADCS7476 12-bit A/D converter is used to measure the voltages at each node. The ADCS7476 can sample up to 1MSPS with ±1 LSB of total unadjusted error from -40^oC to 85^oC and $< \pm 0.2$ LSB of error at 25^oC. No bits are wasted in the ADCS7476 A/D converter. Additionally, the input circuitry to the ADC is a 100Ω resistor in series with a 26pF capacitor. This places a pole at 61MHz, causing a .03% error at 100KHz and .3% error at 1MHz. The additional performance is well worth the additional cost of $1.56375 in quantities of 1Ku.

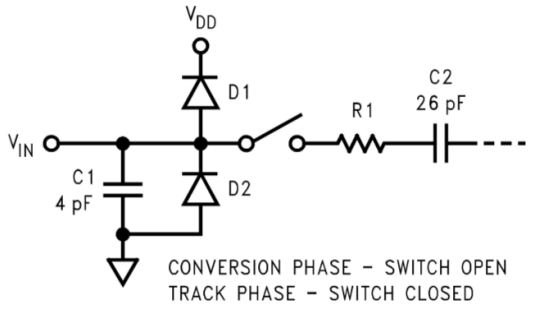

Figure 5-1: ADCS7476 Equivalent Input Circuit

The ADC is connected to the common pin of a CD4051 1:8 analog multiplexer. The multiplexer is connected to eight breadboard rails, which allows the ADC to measure the voltage on any of the eight rails, one rail at a time.

The CD4051 has about 200Ω of series resistance and 30pF of output capacitance when its supply voltage is 12V, which places an additional pole at 26MHz, again well above the Nyquist frequency.

So far, the voltage-reading signal chain has two poles - one at 61MHz and one at 26MHz.

5.3 Signal Generator

The STM32F407 has an onboard D/A converter that is good enough to use as a signal generator. The onboard DAC is configured to output a cosine wavetable with a DC offset, as described in the next chapter.

5.4 Test Voltage Current Sensing

The DAC output is buffered by half of an MCP6L92 10MHz op-amp. The onboard DAC can be configured with an optional onboard buffer, but the buffer limits the DAC output range from 0.2V to Vdd-0.2V. Without the onboard buffer, the DAC output is 15kΩ. When configured as a voltage buffer, the MCP6L92 has an input impedance larger than 1GΩ, resulting in no signal attenuation.

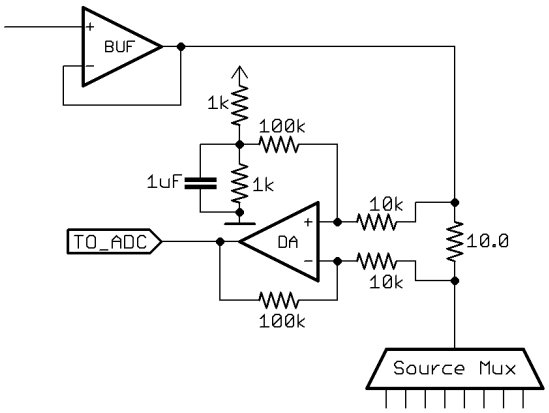

Figure 5-2: Difference Amplifier Schematic

The buffer sources current through a 10.0Ω, 1% sense resistor, which can be switched onto any of the breadboard rails through an array of eight high-side switches. The voltage across the sense resistor is measured by the other half of the MCP6L92 op-amp configured as a simple difference amplifier. Using two 10kΩresistors and two 100kΩresistors, the difference

amplifier is configured with a gain of 10.

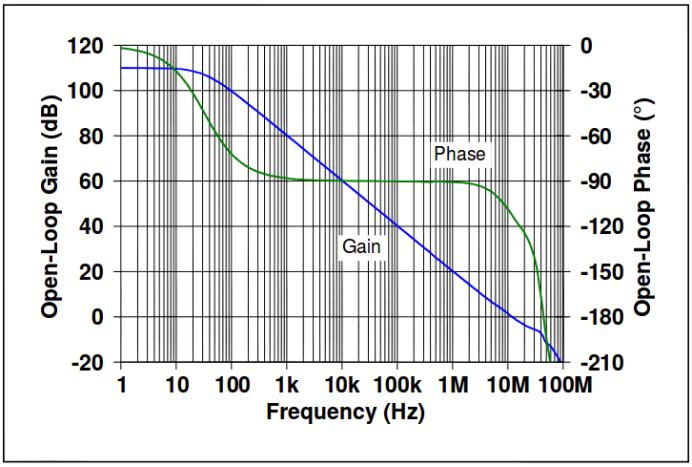

Figure 5-3: MCP6L92 Open Loop Bode Plot

According to the MCP6L92 datasheet, the difference amplifier should have a -3dB bandwidth of 1MHz and plenty of phase margin driving the 100Ω- 26pF input impedance to the current sense ADC.

5.5 High-side Switches

The high-side switches were selected for high-voltage operation, so that any rail of the breadboard could swing between 0 and 30V and there wouldn't be a problem. The selected switches were Vishay DG468 normally open analog switches. They have 9Ωresistance and 76pF of capacitance in the on-state, 1nA of leakage current and 30pF of capacitance in the off-state. The high and low side switches are the main limits of bandwidth due to their high amounts of input capacitance in both on and off states.

5.6 Low-side Switches

The low-side switches have a low logic-level threshold voltage, low drain-source on-resistance, can handle up to 30V, and are low-cost. The IRLML2803 N-FETs have an $R_{DS_{ON}}$ of about 1Ωwith a V_{GS} of 3.3V. With 10V V_{GS}, $R_{DS_{ON}}$ drops to 250mΩ. The downside of these FETs is the high C_{DS} that comes from a wide transistor. C_{DC} is on the order of 60pF for each transistor. When combined with the additional capacitances mentioned above, each breadboard rail has a total of 140pF to ground. This has a significant impact on the maximum usable frequency for even moderate impedances on the breadboard. For example, consider a 10kΩ-10kΩresistor divider. At 100kHz, the 140 pF capacitance on each rail has 11kΩof impedance.

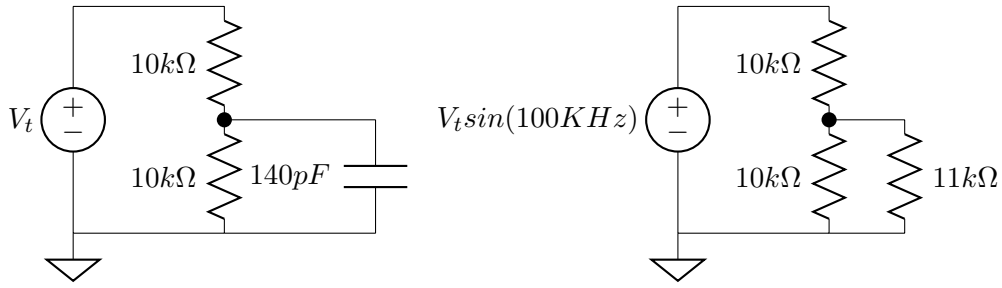

Figure 5-4: Resistor Divider Parasitic Capacitance

5.7 PCB Mounted Breadboard

5.8 Hardware Prototypes

Chapter 6

Firmware

Block Diagram

6.1 ADC

The ADCS7476 is a successive approximation ADC with an SPI interface. In operation, a master device initiates a conversion by pulling $\overline{\texttt{CS}}$ low, then clocks in data using the `CK` line and reading `SDATA`.

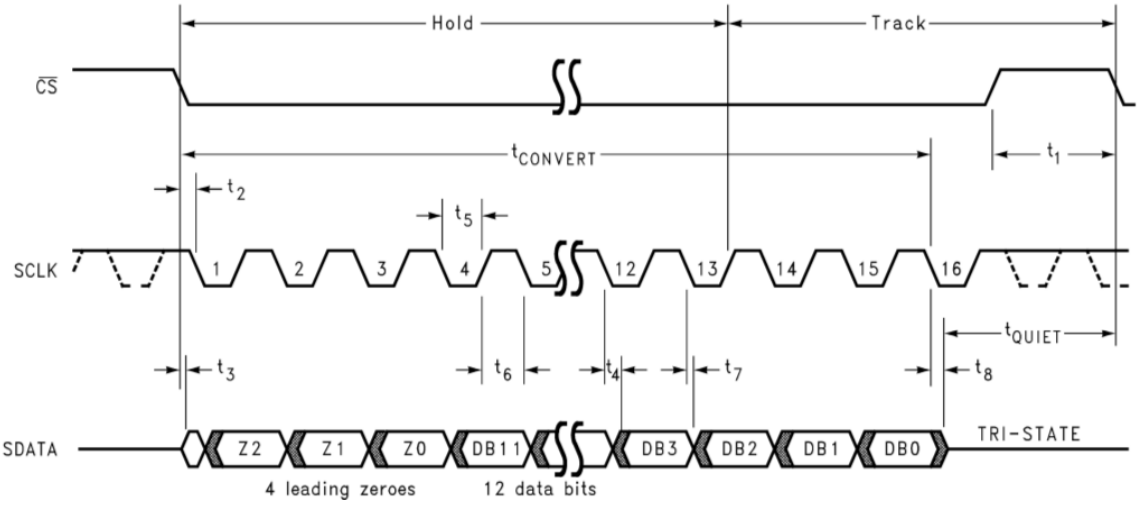

Figure 6-1: ADCS7476 Serial Interface Timing Diagram

The ADC firmware configures two 32-bit timers and the DMA to record data from up to sixteen external ADCs. The two timers are responsible for driving the Chip Select and

Clock lines on all of the ADCs. The timing of the Chip Select line determines the sampling frequency and the Clock line is driven at the ADCS7476's maximum clock frequency of 20MHz. On the rising edge of each clock cycle, the DMA is triggered to sample the data lines of each ADC. A trigger causes the DMA to store each of the 16 pin states on `PORT E` as a 16-bit integer in the buffer `datas`.

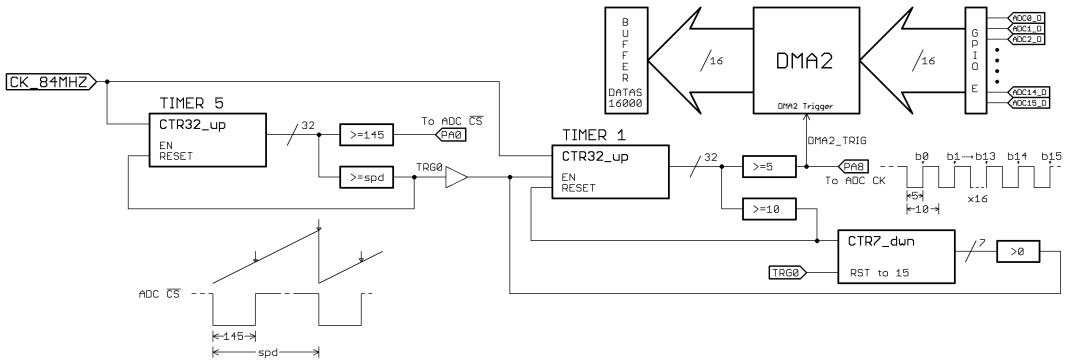

Figure 6-2: Full ADC Driver with DMA

6.1.1 ADC Timers

Timer 5 drives the Chip Select lines. It is configured as a 32-bit up-counting timer clocked at 84MHz, uses output compare unit 1 to control pin PA0 (connected to ADC $\overline{\texttt{CS}}$), and is set to run in continuous mode. The ADC sampling frequency is controlled by the $\overline{\texttt{CS}}$ line, which is controlled by the period of Timer 5. When a host computer requests an ADC trigger, it sends a sampling frequency along with it. The appropriate $\overline{\texttt{CS}}$ period is calculated and assigned to the variable `spd` (sampling period). Timer 5's output compare mode 1 is set to PWM2 mode, where PA0 is low when the counter is less than the compare value and high when the counter is greater than the compare value. At update, Timer 5's count value is reset to 0, so PA0 falls to 0V and initiates a conversion. When Timer 5 counts to 145, $1.7\mu S$ later, the conversion is complete and PA0 rises to 3.3V, until the count reaches `spd` and the cycle starts again. Timer 5 is also configured in Master Mode and sends a trigger

signal on TRG0 at each update event. In this case, the signal on TRG0 is used to enable Timer 1.

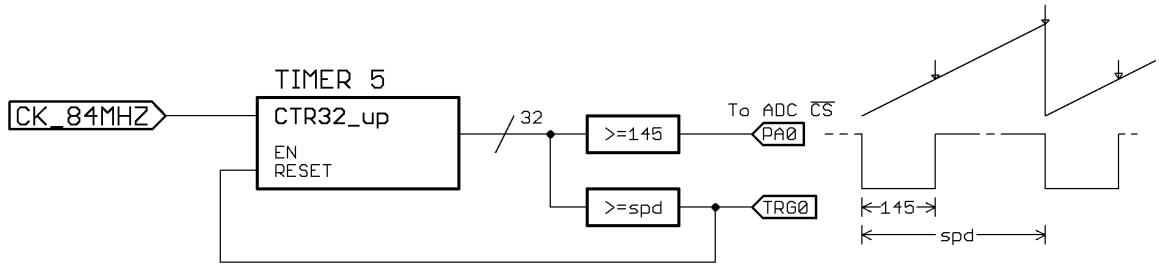

Figure 6-3: ADC Chip Select Timer

Timer 1 drives the ADC Clock lines and behaves as a $1\mu S$ on - $1\mu S$ off 16-shot timer. It's also configured as a 32-bit up-counting timer clocked at 84MHz, but it's only enabled by the TRG0 signal from Timer 5. Like Timer 5, it uses output compare unit 1 to control an output pin, in this case `PA8`. Unlike Timer 5, it's set to run in one-shot mode with a repetition counter that is preloaded with a value of 15. The output compare unit is set to run in PWM2 mode with fixed compare and update registers. When Timer 1 counts to 5, the compare unit fires and PA8 goes high. When the count reaches 10, the timer is updated, PA8 goes low, and the repetition counter decrements. The timer continues to run, toggling PA8 and decrementing the repetition counter, until the repetition counter reaches a value of 0. Once the repetition counter reaches 0, the next Timer 1 update disables the timer.

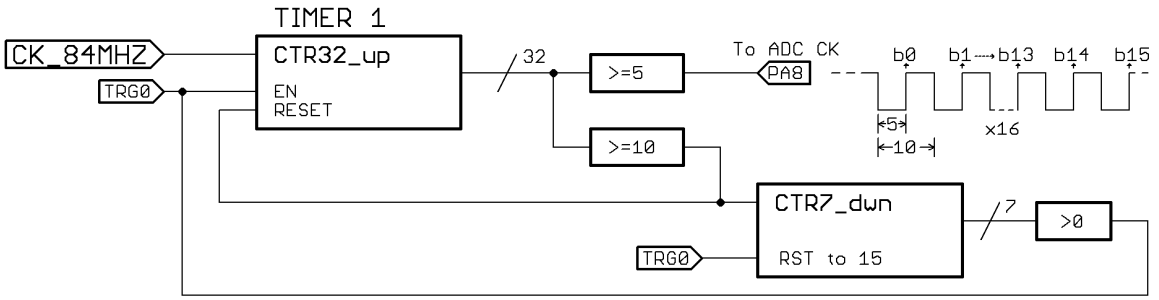

Figure 6-4: ADC Clock Timer

6.1.2 ADC DMA

A DMA controller is used to store serial ADC data from up to 16 ADCs in parallel. On each clock cycle, DMA2 takes the 16-bit integer value represented by the state of the 16 pins on `PORT E` and stores it in memory. As shown in Figure 5.1, the ADC data pin is updated on a falling clock signal. To record the state of the data pin, DMA2 is triggered to start a data transfer on every compare event from Timer 1, which corresponds with the rising edge of the clock signal.

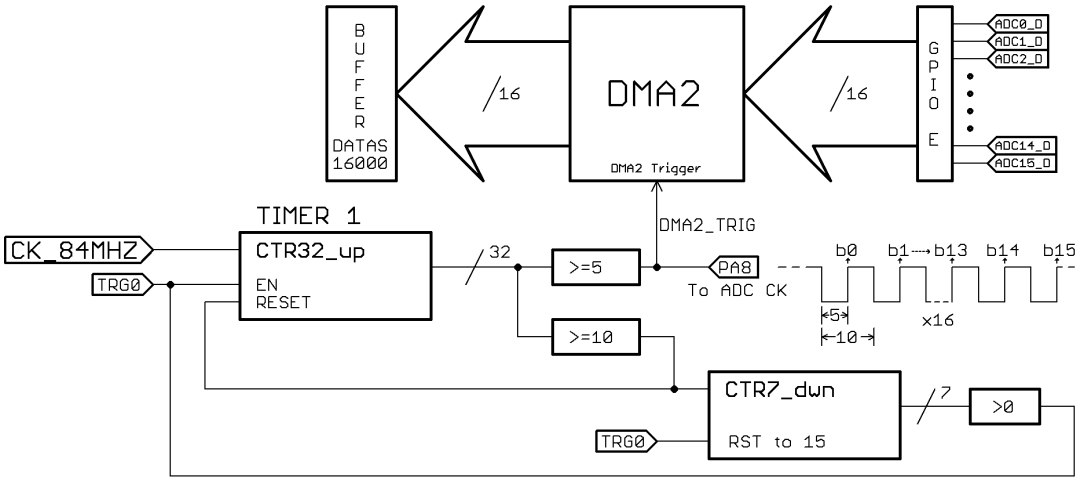

Figure 6-5: ADC Clock Timer Triggers DMA2

When Timer 5 is enabled, DMA2's 'number of data' [to transfer] register is set to 16000 and the ADCs continuously sample at the sample period defined by `spd`. In each cycle of Timer 5, Timer 1 toggles the clock line 16 times, triggering DMA2 on each rising edge. With each DMA trigger, DMA2's number of data register decrements. When the register reaches 0, an interrupt fires that disables Timer 5 and begins the data reconstruction process.

6.1.3 Data Reconstruction

Since the serial data stream from each ADC is stored sequentially, the actual A/D readings need to be reconstructed after they are recorded. In Figure 5-6, the binary data stored in `datas` is examined. Each 16-bit integer in `datas` contains one bit of data from each of the

16 pins on `PORT E`, which connect to the data pins on the external A/D converters. Here, each letter represents the data from a particular external ADC.

Bit Index	b_{15}	b_{14}	b_{13}	b_{12}	...	b_3	b_2	b_1	b_0
`datas[0]`	p_{15}	o_{15}	n_{15}	m_{15}	...	d_{15}	c_{15}	b_{15}	a_{15}
`datas[1]`	p_{14}	o_{14}	n_{14}	m_{14}	...	d_{14}	c_{14}	b_{14}	a_{14}
`datas[2]`	p_{13}	o_{13}	n_{13}	m_{13}	...	d_{13}	c_{13}	b_{13}	a_{13}
`datas[3]`	p_{12}	o_{12}	n_{12}	m_{12}	...	d_{12}	c_{12}	b_{12}	a_{12}
⋮	⋮	⋮	⋮	⋮	...	⋮	⋮	⋮	⋮
`datas[13]`	p_2	o_2	n_2	m_2	...	d_2	c_2	b_2	a_2
`datas[14]`	p_1	o_1	n_1	m_1	...	d_1	c_1	b_1	a_1
`datas[15]`	p_0	o_0	n_0	m_0	...	d_0	c_0	b_0	a_0
`datas[16]`	p_{15}	o_{15}	n_{15}	m_{15}	...	d_{15}	c_{15}	b_{15}	a_{15}

Figure 6-6: `datas[0:16]`

To reconstruct the data collected from $\text{ADC}_a[0]$, a routine iterates through `datas[0:15]`, summing appropriately bit-shifted b_0's.

$\text{ADC}_a[0] = (a_{15} << 15) + (a_{14} << 14) + (a_{13} << 13) + ... + (a_2 << 2) + (a_1 << 1) + a_0$

To reconstruct all of the waveform recorded, the routine iterates through `datas[0:16000]`, reconstructing 1000 samples from each ADC.

6.2 DAC

The STM32F407's onboard DAC is used as a signal source for impedance testing. The DAC is configured to update on a timer, and is fed new waveform values from a wavetable on command. The timer

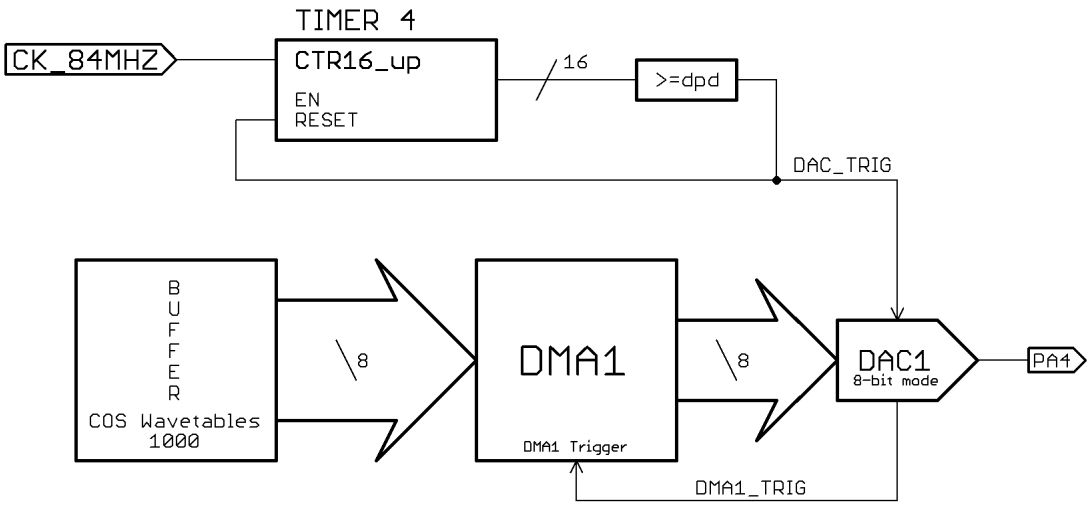

Figure 6-7: DAC Timer Triggers DMA1

6.2.1 DAC Timer

6.2.2 DAC DMA

6.2.3 DAC Wavetables

6.3 USB

6.3.1 USBACM

6.3.2 Command List